Clin Oral Invest (2010) 14:543–549
DOI 10.1007/s00784-009-0334-9

ORIGINAL ARTICLE

Alveolar bone changes under overhanging restorations

Füsun Yasar · Esra Yesilova · Faruk Akgünlü

Received: 4 December 2008 / Accepted: 30 July 2009 / Published online: 18 August 2009

Abstract The aim of this study was to investigate changes in the trabecular architecture of the alveolar bone beneath overhanging restorations with bitewing radiographs in patients having no radiographically visible vertical bone loss. Twenty-eight digital bitewing radiographs with overhanging restorations and 28 digital bitewing radiographs without any restorations belonging to the contralateral side of the same patient were included in the study. Regions of interests (ROI) were created in the alveolar bone along the interproximal regions. These ROIs were segmented to binary images with ImageJ, and, within these binary images, the number of radiographically visible trabecular bone islands per unit area was counted; in addition, the Feret diameter and fractal dimension (FD) were measured. It was found that the mean number of objects per unit area was statistically different in alveolar bone with overhanging restorations from control sites ($p<0.0001$). However, the FeD ($p=0.179$) and FD ($p=0.963$) did not show statistically significant differences between alveolar bone with and without overhanging restorations.

Keywords Overhanging restorations · Alveolar bone · Digital radiography · Image processing · Image analysis

Introduction

Faulty dental restorations and prostheses are common causes of gingival inflammation and periodontal destruction. Overhanging margins provide ideal locations for the accumulation of plaque and result in a change in the ecologic balance of the gingival sulcus region, thereby causing an increase in the amount of disease-associated organisms. However, when these overhangs are removed, the control of plaque can be performed more effectively; gingival inflammation disappears, and alveolar bone support increases [1]. Notably, the prevalence of amalgam overhangs has been well documented in previous studies [2–4].

Despite recent technological advances in restorative dentistry and dental materials, it appears that overhanging margins from restoration procedures still occur. This condition is often neither detected nor eliminated and may be a significant factor in the etiology of periodontal disease [5]. Importantly, a dynamic relationship exists between the periodontium and the tooth [1, 6]. The presence of overhanging amalgam margins in interproximal locations is thought to disturb this relationship and results in a loss of alveolar bone height [4]. It is generally difficult, or sometimes impossible, to examine the contact points and areas on the posterior teeth for the detection of carious lesions or overhanging restorations with conventional clinical examination methods [7]. Hence, the most reliable way of diagnosing overhanging margins is by using a combination of both clinical and radiographic assessments [4, 8].

Overhanging restorations are primarily found in class II restorations [9]. It has been shown that there is a greater loss of periodontal attachment in teeth with overhangs than in those without [4, 10–12]. Bitewing radiographs have been reported to detect more approximal lesions and inadequate restorative treatments of filled surfaces compared to clinical examinations alone [13].

In previous studies, alveolar bone loss associated with overhanging restorations evaluated mean height from the radiographs or measured pocket depth [4, 10–12]. However,

F. Yasar (✉) · E. Yesilova · F. Akgünlü
Oral Diagnosis and Radiology Department, Dentistry Faculty,
Selcuk University,
Alaeddin Keykubat Kampüsü,
Selçuklu, Konya, Turkey
e-mail: drfyasar@hotmail.com

radiographic trabecular bone changes that may accompany overhanging restorations were not studied. In this study, the aim was to evaluate radiographically visible alveolar bone changes in binary images beneath the overhanging restorations in patients without apparent vertical bone loss in the overhanging restoration region.

Materials and methods

Subjects

Twenty-eight digital bitewing radiographs with overhanging restorations and 28 digital bitewing radiographs without any restoration belonging to the contralateral side of the same patient were included in the study. All of the patients had two premolars and two molars on both sides of the jaws and none of the patients had radiographically evident vertical bone loss, especially in the overhanging restoration region. The teeth having overhanging restorations and the control teeth included in the study were among the first and second premolar teeth, as well as the first and second molar teeth of the maxilla and mandible. The radiographs included in the study were chosen from the archives of Oral Diagnosis and Radiology Department and belonged to the patients who came for their routine plaque control. Notably, none of the patients had any systemic disease that would affect bone metabolism. Because this study was performed retrospectively on radiographs from the archives, the definite exposure time of the overhanging restorations was not known. All of the patients were male and were referred to the periodontology department for plaque control. The results of the clinical examinations were not known, but, with respect to the information that was obtained from the treatment plans of the patients, all of them exhibited good oral hygiene, and they were referred to the periodontology department only for plaque control. The radiographs of the patients were evaluated by two observers with a common consensus that the patients did not have vertical bone loss, yet there was an overhanging restoration, and the contralateral tooth was sound and did not have any restoration. When evaluating bone loss, it was accepted that the angulation of the crest for the interdental septum was parallel to a line between the cementoenamel junctions (CEJ) of the approximating teeth, as suggested in the textbook of *Carranza's Clinical Periodontology* [14].

Radiographs

The digital bitewing radiographs were all exposed using the same intraoral X-ray unit (Trophy CCX Digital Periapical X-ray machine, France) with 65 kV, 10 mA, and 2.5 mm equivalent total filtration, and they were acquired with size number 2 Digora phosphor plates. The resolution of the images was set to 8-bit gray levels.

Image analysis

The entire image processing and analyzing were done with ImageJ software (www.rsb.info.nih.gov/ij/). These radiographs were specifically rotated with the arbitrarily rotate command of the program in order to maximize the size of the regions of interest (ROI; Fig. 1). An ROI was chosen in the alveolar bone beneath the overhanging restoration while another ROI was chosen in the contralateral interdental area in the corresponding tooth that had no restoration. These ROIs were segmented to binary images with ImageJ (www.rsb.info.nih.gov/ij/) in a similar way, which has been previously described in a report that evaluated the alterations of the trabecular pattern in patients with osteoporosis [15], as well as in other studies [16, 17]. The ROI was first duplicated and blurred with a Gaussian filter with a diameter of 20, and this blurred version of the image was subtracted from the original image and 128 were added. Later, it was made binary with a threshold level of 128 (Fig. 2). From these binary images, the number of objects (NO) was counted with the analyze particle command of the program. Feret diameters (FeD) for these objects were measured, and the fractal dimension (FD) in the box-counting method was calculated. As the sizes of the ROIs are different from each other because of the differences of the available interdental spaces, the NO was divided by the area of the ROI to generate the mean NO per unit area (MNO/A). Because the mean FeD was used for the calculations, no standardization was applied to it. The angle of the overhanging part of the restoration was also measured and the correlation of this angle with the alveolar bone measurements was evaluated. When measuring the

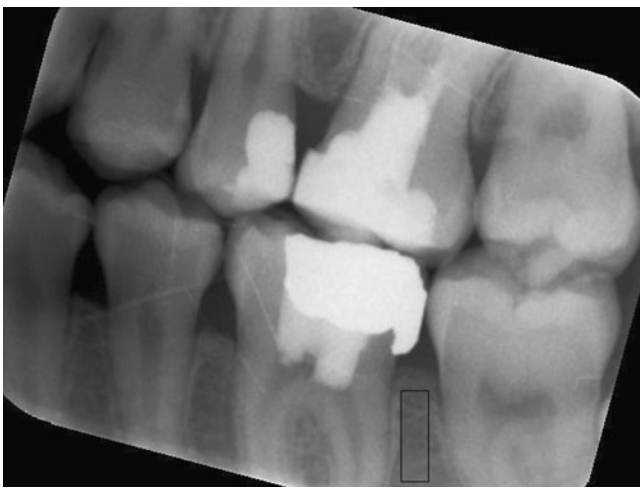

Fig. 1 The placement of ROI in the rotated bitewing radiograph. 45×34 mm (350×350 DPI)

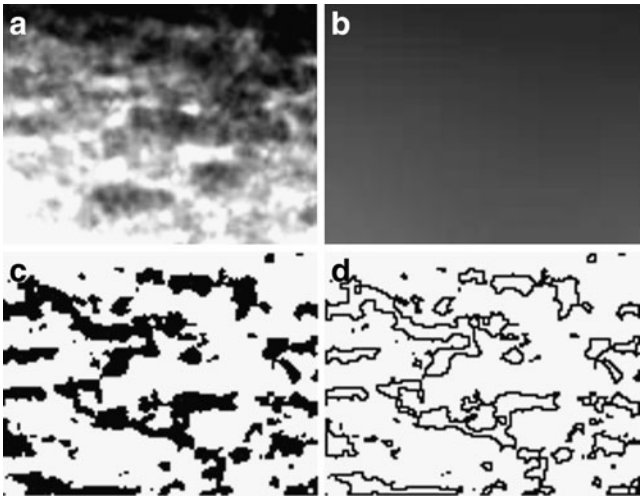

Fig. 2 **a** The original ROI. **b** Blurred version of the ROI with Gaussian filter. **c** Binary form of the image where *black regions* represent trabecular bone. **d** The outlines of trabecular bone. 20×21 mm (350×350 DPI)

angle of the overhanging part of the restoration to the root surface of the tooth, first, a line from the outer part of the restoration to the root surface was drawn. Second, a continuous line on the surface of the root to the root surface restoration union was drawn, and the angle between these two lines was measured (Fig. 3). The distribution of the angles for the overhanging part of the dental restorations is given in Fig. 4. All of the measurements were repeated at least 6 months later in order to evaluate the reproducibility of the measurements. The mean from the repeated measurements was used in the statistical analysis.

Statistical analysis

SPSS 10.0 was used for the statistical analysis. The normality of the data was checked with a Kolmogorov–Smirnov test. The differences between the alveolar bone

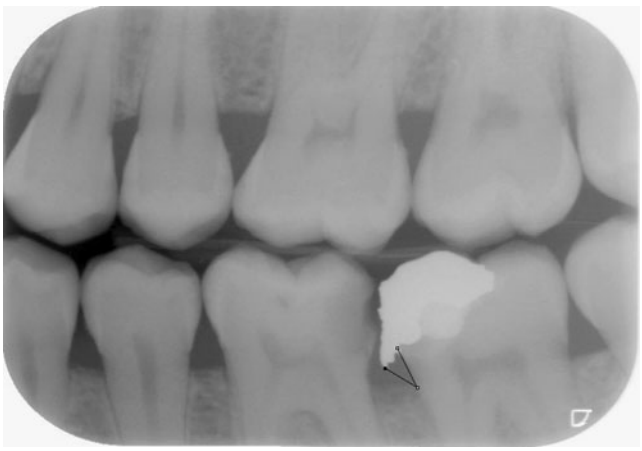

Fig. 3 Measuring the angle of the overhanging part of the restoration to the root surface of the tooth. 56×39 mm (350×350 DPI)

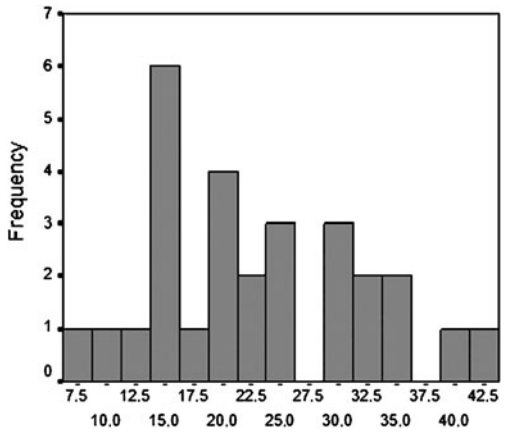

Fig. 4 The distribution of the angles for the overhanging part of the dental restorations. 26×22 mm (350×350 DPI)

with overhanging restorations and control sites were evaluated with a paired-sample *t* test for FD, and the nonparametric Wilcoxon signed ranks test was used to check for the differences between the groups for the MNO/A and mean FeD. In this study, the alpha level (p) was used as 0.05 for the paired-sample *t* test and 0.025 for the Wilcoxon signed rank test. The Bonferroni-corrected p value (p=0.025) was used in Wilcoxon signed rank test because two variables were evaluated together.

Results

Table 1 demonstrates the means, standard deviations, and the standard errors of the variables. The data for the MNO per unit area (MNO/A-1) in areas without restoration (p=0.004) and mean FeD (MFeD-1) in areas without restoration (p=0.040) did not have a normal distribution. It was found that the MNO/A was lower in the alveolar bone under overhanging restorations (0.025) than in control sites (0.054), and there was a statistically significant difference between the MNO/A in the alveolar bone with overhanging restorations and control sites (p<0.0001; Table 1). The MFeD was higher in alveolar bone with overhanging restorations (MFeD for alveolar bone in control sites was 8.749, while the MFeD for alveolar bone with overhanging restoration was 9.369); however, this difference did not reach a statistically significant level (p=0.179; Table 1). There was no statistically significant difference for FD (p=0.963) between sites with and without overhanging restorations (Table 1). Correlations between the angle of the overhanging restoration and MNO/A, MFD, and MFeD were calculated with a Pearson correlation test, and no correlation was found among the variables (Table 2).

The repeatability of the variables was controlled for by calculating Cronbach's alpha, and it was found that the Cronbach's alpha value was 0.15 for the MNO/A-1 (in

Table 1 Mean, standard deviation, and standard error of all recorded parameters (NO/A-1, NO/A-2, FeD-1, FeD-2, FD-1, FD-2, mean angle of the region of overhanging restorations to the alveolar bone, age of the patients)

Variables	Mean		SD	Paired-sample *t* test	Wilcoxon signed ranks test
	Statistic	Std. error		(P=0.05)	(P=0.025)
MNO/A -1	0.054	0.01	0.05		p<0.0001
MNO/A -2	0.025	0.001	0.005		
MFeD-1	8.749	0.225	1.191		p=0.179
MFeD-2	9.369	0.305	1.614		
MFD-1	1.519	0.013	0.071	p=0.963	
MFD-2	1.520	0.019	0.102		
MAngle	23.316	1.723	9.117		
Age	25.428	0.540	2.860		

Comparison of the mean number of trabecular bone islands per unit area (MNO/A-1), the mean FeD (MFeD-1), and mean FD (MFD-1); in sites without restorations and sites with overhanging restorations (MNO/A-2; MFeD-2; MFD-2)

N number of radiographs, *MNO/A-1* the mean NO (trabecular bone islands) per unit area in alveolar bone without restoration (control sites), *MNO/A-2* the mean NO (trabecular bone islands) per unit area in alveolar bone with overhanging restorations, *MFeD-1* mean FeD (the longest diameter) of trabecular bone islands in alveolar bone without restoration (control sites), *MFeD-2* mean FeD (the longest diameter) of trabecular bone islands in alveolar bone with overhanging restorations, *MFD-1* mean FD of alveolar bone without restoration (control sites), *MFD-2* mean FD of alveolar bone with overhanging restorations, *MAngle* mean angle of the overhanging restoration to the alveolar bone

control sites), 0.88 for the MNO/A-2 (in areas with overhanging restorations), 0.47 for FeD-1 (in control sites), 0.71 for FeD-2 (in areas with overhanging restorations), 0.68 for FD-1 (in control sites), 0.94 for FD-2 (in areas with overhanging restorations), and 0.93 for the angle of the overhanging restoration.

Discussion

Overhanging dental restoration is defined as an extension of restorative material beyond the confines of the cavity preparation. These overhangs have been implicated as an etiologic factor in the progression of periodontal disease. They promote plaque accumulation and change nondestructive subgingival flora to destructive strains [18]. However, clinically sound restorations may also be important etiological factors in the initiation of periodontal disease if they are positioned subgingivally [19]. The main objective of this study was to evaluate the changes in the trabecular architecture of the alveolar bone beneath overhanging restorations with bitewing radiographs in patients who presented with no evidence of radiographically visible vertical bone loss. According to Carranza's suggestion, if the distance from the CEJ to the alveolar crest is 2 mm and there are no clinical signs of attachment loss in adolescents, then this is considered to be within the normal limits, and there is typically no associated periodontitis [14]. However, this distance may be greater in older patients [14]. While the normal limit of this distance has been reported to be 2 mm in some textbooks [14, 20], others have reported it to be from 1 to 1.5 mm [21]. Although the bitewing radiographs included in this study were nonstandardized radiographs, all of them were clinically acceptable. In a previous study, it was found that alveolar bone loss in periodontitis or the prevalence of the disease can be accurately and reliably evaluated from nonstandardized bitewing radiographs [22].

Segmented images are formed by gathering their elements into sets likely to be associated with meaningful objects. The goal of segmentation is to simplify the image and reduce it to its basic components [23]. A quantitative, accurate, and reliable method for measuring trabecular bone structure has been the focus of a large body of research, and the validation of some of these methods could prove to have substantial clinical utility [24].

Although there was no radiographically detectable vertical alveolar bone loss, the number of radiographically visible trabecular bone islands was decreased in the alveolar bone beneath the overhangs (p<0.0001). The NO here represents the number of radiographically visible trabecular bone islands. The NO was counted with the ImageJ program's analyze particle command. This command counts and measures objects in binary or thresholded images. It works by scanning the image or selection until it finds the edge of an object. It then outlines the object

Table 2 Correlations between the angle of the overhanging restoration and MNO/A-2, MFD-2, and MFeD-2

		MNO/A-2	MFD-2	MFeD-2
ANGLE	Pearson correlation	−0.211	0.037	0.143
	Sig. (2-tailed)	0.282	0.854	0.468

using the wand tool, measures it using the measure command, fills it to make it invisible, then resumes scanning until it reaches the end of the image or selection [16]. Bland and Altman reported that Cronbach's alpha values of 0.7 to 0.8 are regarded as satisfactory in comparing groups [25]. However, the repeatability of this measurement in control sites was unacceptable (Cronbach's alpha value of 0.15). Counting the objects (bone islands in this study) in digital images within ROIs is a simple measurement. When a new ROI is generated in another place within the same interdental alveolar bone, some particles might be crossed by the edge of the ROI. As a consequence of this, depending on their shape and size, some of the bone islands might be counted twice or more. Hence, this should account for why the NO in the control sites could not be reproduced 6 months later.

An X-ray radiograph is a two-dimensional (2D) projection of a three-dimensional (3D) structure. Various studies have evaluated how this 3D information is reflected in 2D projection radiographs. It was shown that a simple projection provides 3D information about the bone structure [26–28]. In addition, X-ray radiographs were also found to be correlated with bone histomorphometry [29]. FeD is the greatest distance possible between any two points along the boundary of an ROI. In this study, the FeD was the diameter of a radiographically visible trabecular bone island and the maximal FeD was measured [30]. This is a measure of feature size and sometimes called the feature length because it corresponds closely to the longest distance between any two points on the periphery and defines the dimensionality of the figure [30–32] (Fig. 5). Although this measurement has been shown to be useful in histological evaluations [33, 34], there was no statistically

Fig. 5 An example of measuring FeD of the trabecular bone island in the middle of the ROI. The central part of the ROI is magnified, and the *line* shows the FeD of the individual trabecular bone island. 24×23 mm (350×350 DPI)

significant difference (p=0.179) between the mean FeD of the alveolar bone beneath overhanging restorations and control sites in this study. Another caveat is that the FeD might be sensitive to alterations in an object's real size and shape. The sizes and shapes of the individual objects that are contained in the binary radiographs are not in their original form because of the information that was lost during binarization and superimposition of individual trabeculae upon each other. This may limit FeD's applicability in X-ray images. The repeatability of FeD for control and overhanging restoration sites was 0.47 and 0.71, respectively.

FD is a mathematical technique that can aid in the quantification of complex structures. In general, more complex shapes have a higher FD. This technique has been reported to be used with varying degrees of success in different imaging modalities such as plain film radiography, mammography, CT, and MRI [35]. Various investigators have evaluated the structure of the trabecular bone on dental radiographs by using different FD methods with the aim of discriminating individuals with osteoporosis from those without [36, 37]. FD measurements have also been used in discriminating periodontitis [38] and sickle cell anemia patients from healthy ones [39, 40]. In this study, FD could not differentiate alveolar bone changes beneath overhanging restorations versus control sites (p=0.963). The repeatability of FD was 0.68 for control sites and 0.94 for areas with overhanging restorations.

The reliability or amount of noise, among the quantitative trabecular parameters that are typically measured in panoramic and intraoral dental radiographs, was evaluated in a previous study. In those radiographs, some analyses classified as simple geometric, topological, and directional measurement were performed. It was found that 83% of Cronbach's alpha values were at least 0.9, and 99% were at least 0.8. It was also shown that that the proposed trabecular parameters could be measured with a high degree of reproducibility [41]. In this study, it was found that Cronbach's alpha was 0.15 for the MNO/A-1 (in control sites), 0.47 for FeD-1 (in control sites), and 0.68 for FD-1 (in control sites). These values are lower than required to be regarded as satisfactory [25], and this might cause their usage to be questionable. Geraets et al. reported higher Cronbach's alpha values than this study, and the reason for this difference might be due to the variability in the researchers' experience and proficiency in creating ROIs.

It was found that small overhangs, unlike medium and large overhangs, did not result in increased alveolar bone loss around the affected tooth [3]. In another study, overhang width and patient age did not show any statistical correlation with alveolar bone loss [4]. Small overhangs, along with the medium and large overhangs, were also

included in this study, and it was found that the angle of the overhanging restoration relative to the root surface of the tooth did not have any correlation with the other parameters (NO/A, FeD, FD) evaluated. The repeatability for the angle of the overhanging restorations was found to be sufficient (Cronbach's alpha value of 0.93).

Previous studies have examined the effects of overhang removal in terms of Gingival and Plaque Index scores over a period of 3 months, and a reversal of the early radiographic signs of alveolar bone destruction was observed [42]. In addition, the effects of the placement of subgingival restorations with overhanging margins on the subgingival microflora were evaluated in a previous study [43]. The patients included in the study were instructed to continue their normal oral hygiene procedures except that the proximal surfaces of the onlays were to be left uncleaned. Following the placement of the restorations, the percentage of surfaces which bled upon probing gradually increased along with the clinical probing depths starting from the 7th to the 11th week. That study also demonstrated that the placement of restorations with overhanging subgingival margins resulted in a change in the composition of the subgingival microflora at that site, whereby the postprocedural microflora were associated with subsequent periodontitis rather than the presence of increased plaque masses [43]. It was concluded that the overhanging margins of restorations not only facilitated plaque accumulation but also caused an increase in the proportion of anaerobic species of microorganisms [43]. Due to the retrospective design and results of the current study, plaque accumulation was not recorded for test or control sites. Thus, it cannot be concluded that overhanging margins are the solitary cause for the decrease in the number of trabecular bone islands. However, the composition of bacteria is thought to be more important than the total mass, and overhanging restorations are reported to cause an increase in the anaerobic species [43]. Then, in order to conclude that overhanging restorations cause a decrease in the number of trabecular bone islands, not only the amount of plaque but also the composition of it should be known.

Trabecular bone, marrow spaces, and cortical bone constitute the dense portion of alveolar bone in radiographs. It has been reported that the buccal and lingual cortical plates of the mandible and maxilla do not cast a discernible image in periapical radiographs [44]. This means that the trabecular bone mostly contributes to the density of the radiograph, and each structural feature should show a correlation with density [45]. It has been suggested that crestal bone density loss occurs before crestal bone height loss; therefore, radiographic analysis procedures that measure changes in bone density serve as sensitive methods for predicting future loss of crestal bone height [46]. The findings of this study support this suggestion, which indicated that there was a decrease in the number of trabecular bone islands beneath overhanging restorations. MNO/A-1 (the NO in the control sites) did not have a normal distribution, while the mean and standard deviation of this measurement were nearly the same. This cannot be attributed to the negative effect of other factors such as the amount of plaque present or individual inflammatory responses, yet it does show that the data were spread out over a large range of values [47]. The reason for this might be because the number of radiographically visible trabeculae exhibit differences from one patient to another, as well as from one region to another even within the same patient [48]. Other reasons for this might be due to the superimposition of the individual trabeculae in the 2D radiographic images and the information that was lost during binarization. The repeatability of the MNO/A was found to be low in control sites (Cronbach's alpha value was 0.15), and this might be a limitation in its utility. However, overhanging margins of dental restorations seem to cause a decrease in the number of trabecular bone islands, and this might lead to decreases in alveolar bone height over the forthcoming years if the overhangs are not removed.

Conflict of interests The authors declare that they have no conflicts of interest.

References

1. Newman MG, Takei HH, Klokkevold PR, Carranza FA (2007) Carranza's clinical periodontology. The role of dental calculus and other predisposing factors, 10th edn. Saunders/Elsevier, St. Louis, pp 170–192 Middle East and African Edition
2. Gilmore N, Sheiham AJ (1971) Overhanging dental restorations and periodontal disease. Periodontol 42:8–12
3. Jeffcoat MK, Howell TH (1980) Alveolar bone destruction due to overhanging amalgam in periodontal disease. J Periodontol 51:599–602
4. Parsell DE, Streckfus CF, Stewart BM, Buchanan WT (1998) The effect of amalgam overhangs on alveolar bone height as a function of patient age and overhang width. Oper Dent 23:94–99
5. Pack ARC, Coxhead LJ, McDonald BW (1990) The prevalence of overhanging margins in posterior amalgam restorations and periodontal consequences. J Clin Periodontol 17:145–152
6. Thomas BOA (1949) The relationship of operative procedures to the health of the periodontal tissues. JADA 39:522–532
7. Pillai K, Hollist NO (1999) Randomized selection of bitewing radiographs: analysis and clinical thereof. Odonto-stomatol Trop 22:11–14
8. Pack AR (1989) The amalgam overhang dilemma: a review of causes and effects, prevention, and removal. N Z Dent J 85:55–58
9. Matthews DC, Tabesh M (2004) Detection of localized tooth-related factors that predispose to periodontal infections. Periodontol 2000 34:136–150
10. Jansson L, Ehnevid H, Lindskog S, Blomlöf L (1994) Proximal restorations and periodontal status. J Clin Periodontol 21:577–582

11. Roman-Torres CV, Cortelli SC, de Araujo MW, Aquino DR, Cortelli JR (2006) A short-term clinical and microbial evaluation of periodontal therapy associated with amalgam overhang removal. J Periodontol 77:1591–1597
12. Sikri VK, Sikri P (1993) Overhanging interproximal silver amalgam restorations. Prevalence and side-effects. Indian J Dent Res 4:13–16
13. Vaarkamp J, ten Bosch JJ, Verdonschot EH, Bronkhoorst EM (2000) The real performance of bitewing radiography and fiber-optic transillumination in approximal caries diagnosis. J Dent Res 79:1747–1751
14. Newman MG, Takei HH, Klokkevold PR, Carranza FA (2007) Carranza's clinical periodontology. Radiographic aids in the diagnosis of periodontal disease, 10th edn. Saunders/Elsevier, St. Louis, pp 561–578 Middle East and African Edition
15. White SC, Rudolph DJ (1999) Alterations of the trabecular pattern of the jaws in patients with osteoporosis. Oral Surg Oral Med Oral Pathol Oral Radiol Endod 88:628–635
16. Geraets WG, Van der Stelt PF, Netelenbos CJ, Elders PJ (1990) A new method for automatic recognition of the radiographic trabecular pattern. J Bone Miner Res 5:227–233
17. Caligiuri P, Giger ML, Favus MJ, He J (1993) Computerized radiographic analysis of osteoporosis: preliminary evaluation. Radiology 186:471–474
18. Brunsvold MA, Lane JJ (1990) The prevalence of overhanging dental restorations and their relationship to periodontal disease. J Clin Periodontol 17:67–72
19. Leon AR (1977) The periodontium and restorative procedures. A critical review. J Oral Rehabil 4:105–117
20. Whaites E (2003) Essentials of dental radiography and radiology. The periodontal tissues and periodontal disease, 3rd edn. Churchill Livingstone, China, pp 241–253
21. White SC, Pharoah MJ (2004) Oral radiology principles and interpretation. Periodontal diseases, 5th edn. Mosby, St. Louis, pp 314–329
22. Merchant AT, Pitiphat W, Parker J, Joshipura K, Kellerman M, Douglass CW (2004) Can nonstandardized bitewing radiographs be used to assess the presence of alveolar bone loss in epidemiologic studies? Community Dent Oral Epidemiol 32:271–276
23. Mol A (1999) Digital quantitative radiography: tools and toys. Dentomaxillofacial Radiol 28:328–329
24. Jolley L, Majumdar S, Kapila S (2006) Technical factors in fractal analysis of periapical radiographs. Dentomaxillofac Radiol 35:393–397
25. Bland JM, Altman DG (1997) Cronbach's alpha. Br Med J 314:572
26. Jennane R, Harba R, Lemineur G, Bretteil S, Estrade A, Benhamou CL (2007) Estimation of the 3D self-similarity parameter of trabecular bone from its 2D projection. Med Image Anal 11:91–98
27. Luo G, Kinney JH, Kaufman JJ, Haupt D, Chiabrera A, Siffert RS (1999) Relationship between plain radiographic patterns and three dimensional trabecular architecture in the human calcaneus. Osteoporos Int 9:339–345
28. Pothuaud L, Benhamou CL, Porion P, Lespessailles E, Harba R, Levitz P (2000) Fractal dimension of trabecular bone projection texture is related to three dimensional microarchitecture. J Bone Miner Res 15:691–699
29. Chappard D, Guggenbuhl P, Legrand E, Baslé MF, Audran M (2005) Texture analysis of X-ray radiographs is correlated with bone histomorphometry. J Bone Miner Metab 23:24–29
30. Russ JC (1994) The image processing handbook. Image measurements, 2nd edn. CRC, Florida, pp 481–546
31. Francus P (2005) Image analysis, sediments and paleoenvironments Image measurements. Springer, Heidelberg, pp 59–86
32. Kindratenko V (1997) Development and application of image analysis techniques for identification and classification of microscopic particles. Shape analysis part 2. Ph.D. Thesis, University of Antwerp, Belgium, pp 32–37
33. Briguet A, Courdier-Fruh I, Foster M, Meier T, Magyar JP (2004) Histological parameters for the quantitative assessment of muscular dystrophy in the mdx-mouse. Neuromuscul Disord 14:675–682
34. Qin L, Zhang G, Sheng H, Yeung KW, Yeung HY, Chan CW, Cheung WH, Griffith J, Chiu KH, Leung KS (2006) Multiple bioimaging modalities in evaluation of an experimental osteonecrosis induced by a combination of lipopolysaccharide and methylprednisolone. Bone 39:863–871
35. Yaşar F, Akgünlü F (2006) The differences in panoramic mandibular indices and fractal dimension between patients with and without spinal osteoporosis. Dentomaxillofac Radiol 35:1–9
36. Ruttimann UE, Webber RL, Hazelrig JB (1992) Fractal dimension from radiographs of peridental alveolar bone: a possible diagnostic indicator of osteoporosis. Oral Surg Oral Med Oral Pathol 74:98–110
37. Law AN, Bollen AM, Chen SK (1996) Detecting osteoporosis using dental radiographs: a comparison of four methods. JADA 127:1734–1742
38. Updike SX, Nowzari H (2008) Fractal analysis of dental radiographs to detect periodontitis-induced trabecular changes. J Periodontal Res 43:658–664
39. Demirbaş AK, Ergün S, Güneri P, Aktener BO, Boyacioğlu H (2008) Mandibular bone changes in sickle cell anemia: fractal analysis. Oral Surg Oral Med Oral Pathol Oral Radiol Endod 106:e41–e48
40. White SC, Cohen JM, Mourshed FA (2000) Digital analysis of trabecular pattern in jaws of patients with sickle cell anemia. Dentomaxillofac Radiol 29:119–124
41. Geraets WGM, Verheij JGC, van der Stelt PF, Horner K, Lindh C, Nicopoulou-Karayianni K, Jacobs R, Devlin H (2007) Osteoporosis and the general dental practitioner: reliability of some digital dental radiological measures. Community Dent Oral Epidemiol 35:465–471
42. Highfield JE, Powell RN (1978) Effects of removal of posterior overhanging metallic margins of restorations upon the periodontal tissues. J Clin Periodontol 5:169–181
43. Lang NP, Kiel RA, Anderhalden K (1983) Clinical and microbiological effects of subgingival restorations with overhanging or clinically perfect margins. J Clin Periodontol 10(6):563–578
44. White SC, Pharoah MJ (2000) Normal radiographic anatomy. Oral radiology principles and interpretation, 4th edn. Mosby, St. Louis, p 175
45. Veenland JF, Grashuis JL, Weinans H, Ding M, Vrooman HA (2002) Suitability of texture features to assess changes in trabecular bone architecture. Pattern Recogn Lett 23:395–403
46. Matteson SR, Deahl ST, Alder ME, Nummikoski PV (1996) Advanced imaging methods. Crit Rev Oral Biol Med 7(4):346–395
47. Mullee MA (1995) How to do it 2: how to choose and use a calculator. BMJ, London, pp 58–62
48. White SC, Pharoah MJ (2004) Oral radiology principles and interpretation. Normal radiographic anatomy, 5th edn. Mosby, St. Louis, p 170